

Using CFD Simulation and Porous Medium Analogy to Assess Cerebral Aneurysm Hemodynamics after Endovascular Embolization

Mohammad O. Hamdan¹, Hashem M. Alargha², Emad Elnajjar², Ali Hilal-Alnaqbi², Waseem H. Aziz^{3,4}

¹American University of Sharjah
P.O. Box 24444, Mechanical Engineering Department, Sharjah, UAE
mhamdan@aus.edu

²United Arab Emirates University
P.O. Box 15551, Mechanical Engineering Department, AlAin, UAE

³Tawam Hospital
Neurosurgery Department, AlAin, UAE

⁴Alexandria University
Department of Neurosurgery, Alexandria, Egypt

Abstract - A numerical analysis is carried out using ANSYS fluent tool to assess coil size and compactness value on unruptured aneurysm after coiling treatment. The study reports the effect of endovascular embolization on blood hemodynamics inside unruptured aneurysm. The coiled aneurysm is model as porous volume with porosity and permeability related to the coil size and compactness value. The results show as coil compactness increases and coil diameter decreases, the blood inflow to aneurysm volume decreases. The reduction in blood inflow to the aneurysm reduces the risk of aneurysm rupture. Also, it reduces flow circulation with the aneurysm and promote thromboses which seals aneurysm.

Keywords: Hemodynamics; Porous medium; Darcy flow; Numerical simulation; Wall shear stress.

1. Introduction

In recent years, CFD analysis became a popular tool to analyze cerebral aneurysm [1-3]. Cerebral aneurysm, is considered a vascular disorder where a local growth of an intracranial artery occurs. It is considered a serious medical condition that could cause death. The growth in cerebral aneurysm may compress surrounding cerebral tissues possibly causing dangerous health conditions. The rupture of a cerebral aneurysm is considered fatal condition [4].

CFD simulation has shown high quantitative agreement with experimental PIV data in terms of similarity index and velocity magnitude [5]. The CFD simulation can provides more detailed information regarding the vascular hemodynamics in cerebral aneurysm [1, 6], coronary artery [7] and in various bio-medical applications [8, 9].

One of the treatment methods of cerebral aneurysm is filling the aneurysm by coil mesh, which is known medically by endovascular embolization. This treatment method is consider the least invasive way of treatment. The coils are introduced to the aneurysm through a catheter implanted into a vessel over the knee, which is navigated through the blood vessels to until it reaches the aneurysm. Thrombogenic, coils are used to form a blood clot around it and reduces the blood flow to the aneurysm, hence, reducing aneurysm rupture occurrence.

In this study, porous media model is used to simulate the coiled aneurysm. In literature, porous medium has been implemented to model aneurysm coiling [10, 11] and to model aneurysm diverting stent [12-14]. The current CFD study utilized the porous media parameters to assess the effect of coil parameters, mainly coil diameter and coil compactness, on the blood hemodynamics. The study reports how WSS changes as function of coil parameters after aneurysm endovascular coiling.

2. Problem Formulation

A schematic of idealized terminal-type bifurcations aneurysm is as shown Figure 1. For clinical purposes, it is recommended to use a patient specific geometry. However, the use of idealized aneurysm in this study aims to provide guidance and direction on predicting the hemodynamics behavior, coiling compactness and coil size. The terminal-type

bifurcations aneurysm model shown in Figure 1b is divided into three sections of interest, the aneurysm dome, the parent artery and the daughter arteries. The repetitive impingement against the vessel wall under pulsatile flows may induce fatigue causing initiation and growth of aneurysms [15].

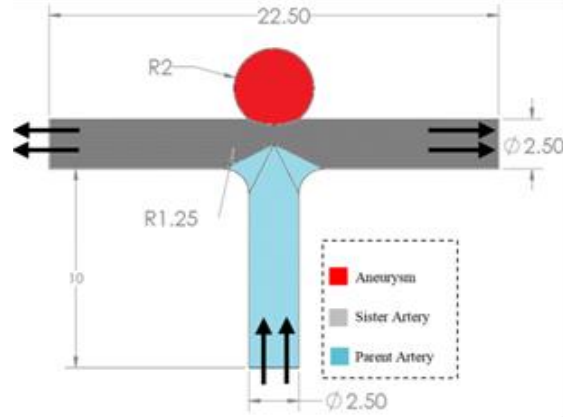


Fig. 1: A schematic of idealized geometry of terminal-type bifurcations aneurysm.

The main artery and the outlet arteries are modeled as pipes with a radius of $r = 1.25 \text{ mm}$ and length of $l = 10 \text{ mm}$. The outlet arteries are bifurcating from the main artery and are given the same radius as the parent artery since such arteries settings have been observed in clinical patient angiography images. The aneurysm is approximated as a spherical shape with radius of $r_a = 3 \text{ mm}$ is created at the apex of the bifurcation as shown in Figure 1.

The coiled mesh is modeled as an isotropic porous media. Porous media is widely used in the literature [16-20]. Porosity is considered isotropic when it is uniform in all orientations. Using this assumption, the equation solved by Fluent for momentum conservation is taken as follow [21]:

$$\frac{\partial(\varepsilon p)}{\partial x} = -\frac{\partial}{\partial x}(\varepsilon \rho v_i v_i) + \frac{\partial(\varepsilon \tau_i)}{\partial x} - \left(D \mu v_i + C \frac{1}{2} \rho v_i v_i \right) \quad (1)$$

Where, ε is porosity, p is pressure, x is independent coordinate variable, v_i is the velocity tensor, ρ is the fluid density, τ_i is the stress tensor and μ is dynamic viscosity. Note that D is the viscous resistance matrix and C is the inertial resistance matrix. These variables are defined as follow:

$$D = \frac{\varepsilon^2}{K} \quad (2)$$

$$C = \frac{2\varepsilon^3 c_f}{\sqrt{K}} \quad (3)$$

The Forchheimer term (inertial resistance matrix) in equation (3) represents the fluid inertial loss due to the impact between fluid and porous matrix. In this study, since fluid circulation inside the aneurysm is very small, the Forchheimer term can be neglected without effecting to the result's accuracy. Hence, the value of C is to zero.

The porosity of a porous region is given by:

$$\varepsilon = \frac{V_{void}}{V_{total}} \quad (4)$$

The endovascular coils permeability (K) is calculated using fibrous relation [22] as shown below:

$$\frac{K}{a^2} = 0.491 \left(\sqrt{\frac{1 - 0.0743}{1 - \varepsilon}} - 1 \right)^{2.31} \quad (5)$$

Where, a is the radius of the fiber (coil).

The blood density has been set to 1050 kg/m^3 while blood viscosity was modeled using the Carreau non-Newtonian viscosity model [23] shown in below equation:

$$\mu = 0.056 + 0.0525 [1 + 10.976 \dot{\gamma}^2]^{-0.3216} \quad (6)$$

Where $\dot{\gamma}$ is rate of strain.

The study focuses on understanding the effect of different common medical coils as shown in Table 1 and Table 2. The analogy between coiled aneurysm and porous media is established by calculating the porosity and permeability of the coiled aneurysm.

Table 1: Different porosity values for coil with radius of $171.45 \mu\text{m}$.

#	Radius [μm]	Porosity	Permeability, K [m^2]	Viscous resistance term, D , [m^{-2}]
1	171.45	0.1	7.75E-13	1.29E+10
2		0.2	3.72E-11	1.08E+09
3		0.3	1.80E-10	4.99E+08
4		0.5	1.37E-09	1.83E+08
5		0.7	7.58E-09	6.47E+07
6		0.9	7.51E-08	1.08E+07

Table 2: Different coils with fixed porosity value/

#	Radius [μm]	Porosity	Permeability, K [m^2]	Viscous resistance term [m^{-2}]
1	133.35	0.6	1.94E-09	1.86E+08
2	152.4		2.53E-09	1.42E+08
3	171.45		3.20E-09	1.12E+08
4	190.5		3.96E-09	9.10E+07
5	254.0		7.03E-09	5.12E+07

3. Numerical Solution

The CFD mesh used in this study has been selected based on mesh independent study shown in Figure 2. By observing the value of WSS for different meshes as shown Figure 2, the mesh with 1.2 million nodes has been used in this study.

The QUICK scheme is used to discretize the conservation equations while the pressure-velocity coupling is realized using the SIMPLEC method with the standard under-relaxation parameters. The convergence residuals criteria are set to 1×10^{-7} for all flow variables.

As suggested by Sinnott et al. [24], transient sine wave inlet velocity model is used to describe the blood velocity with a maximum velocity of 0.5 m/s and 0.5 seconds time period (which represents a pulse rate of 120 pulses per minute).

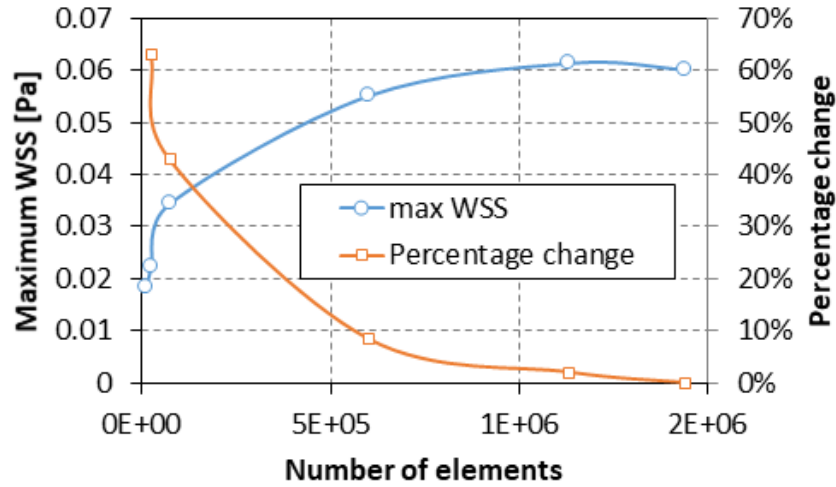


Fig. 2: Maximum WSS and percentage change at the aneurysm dome versus number of elements.

4. Results and Discussion

The impact of coil parameters on blood inflow entering to the aneurysm is explored numerically under multiple coil compactness and for different coils diameter. The coil compactness is related to aneurysm porosity through following relation $\phi = 1 - \epsilon$. Using same coil diameter as indicated in Table 2, the impact of porosity is investigated on aneurysm inflow as shown in Figure 3 and 4.

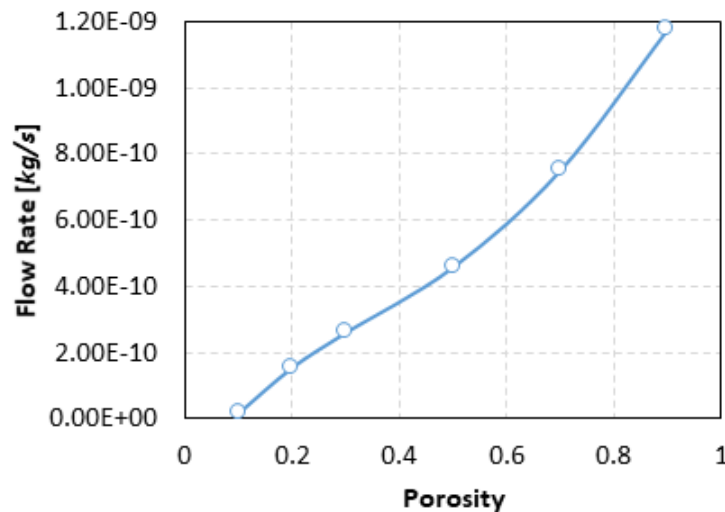


Fig. 3: Flow rate versus aneurysm porosity after coiling with 171.45 μm radius coils.

As shown in Figure 3 as porosity increases from 0.1 (very dense domain) up to 0.9, the inflow rate crossing to the aneurysm increases which is expected since the coils increase the viscous force impacting the flow and reduces the average inflow velocity which lead to lower blood circulation in the aneurysm. Lower blood circulation promote clot formation in the aneurysm and provide proper sealing of the aneurysm.

At fixed coil compactness of 40% (0.6 porosity), as coil radius increases the wall friction decreases, which lead to more inflow to enter the aneurysm as shown in Figure 4. At fixed porosity, as radius increases the surface area to volume ratio will decrease which leads to lower shear forces. As the flow face less shear forces, a higher blood flow is expected and found in Figure 4. The increase in blood inflow to the aneurysm reduces the chance of clot formation which increase the risk of aneurysm rupture.

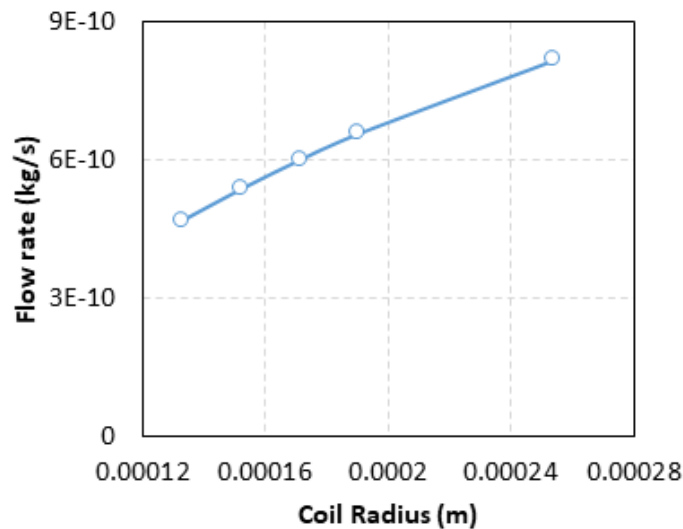


Fig. 4. Flow rate versus coil radius for aneurysm coil compactness of 90% ($\epsilon = 0.1$).

4. Conclusion

This study shows that porous media analogy can provide needed information related the size of coils needed in endovascular embolization. The results show that to assure the effectiveness of coiling treatment, the coiling compactness needs to be as high as 90% (0.1 porosity). Also, for porosity of 60% (compactness of 0.4), the CFD results show that smaller coil diameter causes less flow circulation within the aneurysm, which is desired since it increases the chances of thrombosis.

References

- [1] H. M. AlArgha, M. O. Hamdan, A. Elshawarby, and W. H. Aziz, "CFD Sensitivity study for Newtonian viscosity model in cerebral aneurysms," presented at the *Eleventh International Conference on Computational Fluid Dynamics in the Minerals and Process Industries*, Melbourne, Australia, 2015.
- [2] H. M. AlArgha, M. O. Hamdan, and W. H. Aziz, "Numerical Study on the Hazards of Gravitational Forces on Cerebral Aneurysms," *International Journal of Mechanical, Aerospace, Industrial, Mechatronic and Manufacturing Engineering*, vol. 10, pp. 948-954, 2016.
- [3] D. F. Kallmes, "Point: CFD—computational fluid dynamics or confounding factor dissemination," *American Journal of Neuroradiology*, vol. 33, pp. 395-396, 2012.
- [4] T. Otani, M. Nakamura, T. Fujinaka, M. Hirata, J. Kuroda, K. Shibano, et al., "Computational fluid dynamics of blood flow in coil-embolized aneurysms: effect of packing density on flow stagnation in an idealized geometry," *Medical & Biological Engineering & Computing*, vol. 51, pp. 901-910, 2013.
- [5] C. Roloff, D. Stucht, O. Beuing, and P. Berg, "Comparison of intracranial aneurysm flow quantification techniques: standard PIV vs stereoscopic PIV vs tomographic PIV vs phase-contrast MRI vs CFD," *Journal of neurointerventional surgery*, 2018.

- [6] C. Karmonik, Y. J. Zhang, O. Diaz, R. Klucznik, S. Partovi, R. G. Grossman, et al., "Magnetic resonance imaging as a tool to assess reliability in simulating hemodynamics in cerebral aneurysms with a dedicated computational fluid dynamics prototype: preliminary results," *Cardiovascular diagnosis and therapy*, vol. 4, pp. 207, 2014.
- [7] C. A. Taylor, T. A. Fonte, and J. K. Min, "Computational fluid dynamics applied to cardiac computed tomography for noninvasive quantification of fractional flow reserve: scientific basis," *Journal of the American College of Cardiology*, vol. 61, pp. 2233-2241, 2013.
- [8] D. C. M. Vyas, S. Kumar, and A. Srivastava, "Porous media based bio-heat transfer analysis on counter-current artery vein tissue phantoms: Applications in photo thermal therapy," *International Journal of Heat and Mass Transfer*, vol. 99, pp. 122-140, 2016.
- [9] A. Nakayama and F. Kuwahara, "A general bioheat transfer model based on the theory of porous media," *International Journal of Heat and Mass Transfer*, vol. 51, pp. 3190-3199, 2008.
- [10] Y. Umeda, F. Ishida, M. Tsuji, K. Furukawa, M. Shiba, R. Yasuda, et al., "Computational fluid dynamics (CFD) using porous media modeling predicts recurrence after coiling of cerebral aneurysms," *PloS one*, vol. 12, pp. e0190222, 2017.
- [11] A. Y. Usmani and S. Patel, "Hemodynamics of a Cerebral Aneurysm under Rest and Exercise Conditions," *International Journal of Energy for a Clean Environment*, vol. 19, 2018.
- [12] Y. Li, M. Zhang, D. I. Verrelli, W. Chong, M. Ohta, and Y. Qian, "Numerical simulation of aneurysmal haemodynamics with calibrated porous-medium models of flow-diverting stents," *Journal of biomechanics*, 2018.
- [13] C. Karmonik, J. Anderson, J. Beilner, J. Ge, S. Partovi, R. P. Klucznik, et al., "Relationships and redundancies of selected hemodynamic and structural parameters for characterizing virtual treatment of cerebral aneurysms with flow diverter devices," *Journal of biomechanics*, vol. 49, pp. 2112-2117, 2016.
- [14] P. Bouillot, O. Brina, R. Ouared, K.-O. Lovblad, M. Farhat, and V. M. Pereira, "Hemodynamic transition driven by stent porosity in sidewall aneurysms," *Journal of biomechanics*, vol. 48, pp. 1300-1309, 2015.
- [15] W. Jeong and K. Rhee, "Hemodynamics of cerebral aneurysms: computational analyses of aneurysm progress and treatment," *Computational and mathematical methods in medicine*, vol. 2012, 2012.
- [16] M. O. Hamdan, "An empirical correlation for isothermal parallel plate channel completely filled with porous media," *Thermal Science*, vol. 17, pp. 1061-1070, 2013.
- [17] M. Hamdan and A.-N. Moh'd A, "The use of porous fins for heat transfer augmentation in parallel-plate channels," *Transport in porous media*, vol. 84, pp. 409-420, 2010.
- [18] M. Alkam, M. Al-Nimr, and M. Hamdan, "Enhancing heat transfer in parallel-plate channels by using porous inserts," *International Journal of Heat and Mass Transfer*, vol. 44, pp. 931-938, 2001.
- [19] M. Alkam, M. Al-Nimr, and M. Hamdan, "On forced convection in channels partially filled with porous substrates," *Heat and Mass Transfer*, vol. 38, pp. 337-342, 2002.
- [20] M. Hamdan, M. Al-Nimr, and M. Alkam, "Enhancing forced convection by inserting porous substrate in the core of a parallel-plate channel," *International Journal of Numerical Methods for Heat & Fluid Flow*, vol. 10, pp. 502-518, 2000.
- [21] I. ANSYS, *ANSYS Fluent User's Guide*. 275 Technology Drive Canonsburg, PA 15317: Southpointe, 2013.
- [22] A. Nabovati, E. W. Llewellyn, and A. C. Sousa, "A general model for the permeability of fibrous porous media based on fluid flow simulations using the lattice Boltzmann method," *Composites Part A: Applied Science and Manufacturing*, vol. 40, pp. 860-869, 2009.
- [23] M. W. Siebert and P. S. Fodor, "Newtonian and non-newtonian blood flow over a backward-facing step—a case study," in *Proceedings of the COMSOL Conference*, Boston, 2009.
- [24] M. Sinnott, P. W. Cleary, and M. Prakash, "An investigation of pulsatile blood flow in a bifurcation artery using a grid-free method," in *Proc. Fifth International Conference on CFD in the Process Industries*, 2006.